

# Effect of Corner Angle on Laser Scribing Width and Depth of Al<sub>2</sub>O<sub>3</sub> Ceramics: Experiment and Numerical Simulation

Kaijin Huang<sup>\*,\*\*,\*\*\*,\*\*\*\*,\*\*\*\*\*</sup>, Shu Wang<sup>\*\*\*</sup>, Xin Lin<sup>\*\*\*\*\*</sup>, Xian Chen<sup>\*\*</sup>, Haisong Huang<sup>\*</sup>, Shihao Tang<sup>\*</sup> and Feilong Du<sup>\*</sup>

<sup>\*</sup> Key Laboratory of Advanced Manufacturing Technology, Ministry of Education, Guizhou University, Guiyang 550025, P.R.China  
E-mail: huangkaijin@hust.edu.cn

<sup>\*\*</sup> Zhejiang Provincial Key Laboratory of Laser Processing Robot/ Key Laboratory of Laser Precision Processing & Detection, Wenzhou University, Wenzhou 325035, P.R. China

<sup>\*\*\*</sup> State Key Laboratory of Materials Processing and Die & Mould Technology, Huazhong University of Science and Technology, Wuhan 430074, P.R. China

<sup>\*\*\*\*</sup> Xi'an Technological University, Shaanxi Key Laboratory of Non-Traditional Machining, Xi'an 710021, P.R. China

<sup>\*\*\*\*\*</sup> State Key Laboratory of Solidification Processing, Northwestern Polytechnic University, Xi'an 710072, P. R. China

Laser scribing is a promising micromachining technique for the precision production of complex shapes like corner angle geometry on hard and brittle materials such as silicon, ceramics and glasses. The accuracy and quality of laser scribing depends on the operating parameters and geometries. In this paper, the effect of corner angle on the groove width and depth obtained on Al<sub>2</sub>O<sub>3</sub> samples was studied experimentally, using Diode Pumped Solid State Laser Scribe, and simulated using ANSYS software. The experimental and calculated results all proved that the corner angle had important effect on the accuracy and quality of laser scribing due to the exist of heat accumulation effect and corner angle effect. A decrease of corner angle caused an increase of the groove width and depth on Al<sub>2</sub>O<sub>3</sub>. In addition, the laser scribing time also had important effect on the groove width and depth due to heat accumulation effect, and an increase of laser scribing time caused an increase of the groove width and depth on Al<sub>2</sub>O<sub>3</sub>.

DOI: 10.2961/jlmn.2018.03.0009

**Keywords:** laser scribing, Al<sub>2</sub>O<sub>3</sub> ceramics, heat accumulation effect, corner angle effect, numerical simulation

## 1. Introduction

It is well known that hard and brittle ceramic materials such as Al<sub>2</sub>O<sub>3</sub> and AlN are widely used in the field of electronics industry. However, they are very difficult to process by the use of traditional mechanical method due to their high brittleness and high hardness, especially for complex irregular shapes.

With the development of laser technology, laser precision machining has attracted much attention due to the advantages of non-contact, high-speed and low cost [1] of the process, as well as the ability to obtain complex shapes such as corner angle [2], circular arc [3] and curves [4]. Among these technologies, laser scribing of hard and brittle ceramic materials such as Al<sub>2</sub>O<sub>3</sub> [5] and AlN [6,7] has been widely used in the electronics industry. Iwai et al. [5] investigated the micro scribing of Al<sub>2</sub>O<sub>3</sub> with a diode-pumped Nd:YLF laser. They found that the focal position, wavelength and feed rate of the laser, as well as the number of laser scans, had important effects on the groove width and depth, and the height of Al<sub>2</sub>O<sub>3</sub> debris. Takahashi et al. [6] found that when an AlN ceramic was scribed with a CO<sub>2</sub> laser, the surface resistance was degraded. Tsai et al. [8] developed a new laser machining technique for alumina shaping, based on the principles of fracture mechanics. The fracture machining technique can be applied to shape any

geometry, such as rectangular and quarter-circular corners; however, to obtain the desired contour, the CW Nd:YAG laser must be used to scribe and confine the fracture region. As to the mechanism of groove formation, there are two main mechanisms: melting-evaporation [9-11] and heat induced crack [12, 13]. For example, Xie et al. [9] thinks that it is mainly photothermal effect and the effect results in melting, vaporization, which is essential to the materials removal when a pulsed green laser with wavelength of 532nm is employed to scribe the sapphire substrate. Chen et al. [10] thinks that it is a mixed photothermal and photochemical process for sapphire and a photothermal process for silicon when a near ultraviolet Nd:YAG laser was used to cutting, marking and surface ablation of sapphire and silicon. Iwai et al. [11] thinks that it is thermal effect when a diode-pumped Nd:YLF laser was used to scribe Al<sub>2</sub>O<sub>3</sub> ceramics. Xu et al. [12] believes that laser induced thermal stress is the main mechanism of laser grooving on sapphire wafer. Tsai et al. [13] proposed that the high temperature gradient induced microcrack formation and the material removal is due to the linkage of the groove-cracks when a CO<sub>2</sub> laser and a Nd:YAG laser is employed for step shaping and blind corner shaping for a thick alumina ceramic substrate.

So far, the investigation of laser ceramics scribing has been mainly focused on the optimization of process parameters [5,14-18] and theoretical simulations of the procedure [7,19,20]. Few works have reported the effect of geometry on groove width and depth [21-23]; however, many studies have focused on the effect of the laser cutting corner angle on the quality of the cuts achieved on different materials, such as ceramics [24,25] and steel [1,26-31]. For example, Yilbas et al. [24] studied the laser cutting of a rectangular shape into alumina and found high residual stress values in the corner region when temperatures are high. In addition, in correspondence of the mid-thickness region of the work piece, a high von Mises stress value, of 3.1 GPa, resulted in striation patterns at the cut surface. When laser cutting a triangle into alumina, Yilbas et al. [25] found that the von Mises stress reaches high values at the corners, due to high cooling rates, and that striation patterns formed at the kerf surface. In another study, the same authors [1] examined, through experiments and simulations, the laser cutting of sharp corners of 30.5 and 120.5° on a mild steel sheet of 5 mm thickness. They found residual stresses of 170 and 90 MPa in correspondence of the 30.5° and 120.5° angles, respectively; and that burning occurs around the sharp edges. Deng et al. [26] studied the burning rate of different angles, all of which  $\leq 30^\circ$ , on low-carbon and medium-carbon steel. They found that with angles  $\leq 30^\circ$ , a circular cutting trajectory through the vertex angle can significantly reduce the burning rate. Wu et al. [27] investigated the influence of cutting parameters, such as cutting speed, corner size and laser power, on the thermal stress field through ANSYS simulations and experiments. They found that when the corner size decreases, the issue of heat accumulation becomes more serious, temperature changes more slowly, corner burning rate increases, and thermal stress is reduced. The same effects are obtained when cutting speed is decreased or laser power increased. Zhou et al. [28] investigated the collapse of corners during laser wire-electrode cutting. They found that the intersecting transition algorithm can lead to a higher angle cutting precision than the automatic arc transition algorithm. In addition, the former technique had an angle error,  $f$ , of 0.02 mm with a 150° angle. The angle error decreased with increasing angles. Yilbas et al. [29] investigated the laser cutting of rectangular holes into thick steel sheets. They found the effect of cutting speed on residual stress and temperature levels to be negligible, and that the residual stress was larger in the corners than in other regions of the cut. In any case, the maximum residual stress, found in correspondence of corners, was approximately 180 MPa, lower than the elastic limit of steel. Seebach et al. [30] studied the cutting quality of laser fusion in terms of dross formation of stainless steel. A 90° corner was cut in thick stainless steel, it was found that changing the travel speed (decreased from travel speed  $V$  to 0 first and then increased from 0 to travel speed  $V$  at 90° corner) leads to a finer cutting quality. Ahn et al. [31] carried out a sharp corner cutting of a low carbon (CSP 1N) sheet using a Nd:YAG laser with a continuous wave and investigated the relationship between the corner angle and the loop on the melted area. They found that the extent of the melted region is negligible when the corner angle is of 150°, and that decreasing the angle led to an increase in the

melted area, which means an obvious burning of the work piece.

The application of laser scribing to ceramics presents more complications compared to steel [8,13,32-34]. For example, in the laser shaping of any shape ceramic machining method invented by Tsai et al. [8,13], it is necessary to use focused Nd:YAG laser to scribe a groove-crack first. Then the laser-induced thermal stress is produced by the defocused CO<sub>2</sub> laser and makes the groove-crack extend through the Al<sub>2</sub>O<sub>3</sub> ceramic substrate to obtain the required geometric ceramic objects, in which the laser sharp angle ceramic scribing is involved. Wang et al. [33] reported the mechanism of bulk spalling and melt sputtering based on alumina ceramics, and realized the laser engraving of real three-dimensional ceramic objects with different sizes of pentagram shapes. This also involves laser ceramic sharp angle scribing. Different corner angles will cause different degrees of heat accumulation, affecting the groove width and depth, which, in turn, affect the geometric accuracy of laser precision scribing. Research on this topic is therefore important to determine the applicability of the process. This is the motivation to carry out the research on the content of this paper.

In this paper, the effect of corner angle on the groove width and depth obtained on Al<sub>2</sub>O<sub>3</sub> through laser scribing was simulated using ANSYS software and verified experimentally with the Diode Pumped Solid State (DPSS) Laser Scriber.

## 2. Experimental

The corner angle was scribed on Al<sub>2</sub>O<sub>3</sub> ceramics using RF-P50S DPSS laser ( $\lambda=1.064\mu\text{m}$ ) produced by Ruifeng Photoelectric Technology Company Limited in Wuhan, China. The microsecond semiconductor pumped laser for laser scribing ceramics used in this paper is small in size, light in weight, long in life, simple in structure and low in price, which is beneficial to widely used in developing countries like China. Scribing angles of 15° (sample A) and 60° (sample B), and substrate sizes of 5×5×0.46 mm<sup>3</sup> (L×W×H) are used. The scribing length is 2.5 mm + 2.5 mm (L/2 + W/2). The groove width and depth were measured with the VHX-1000 three-dimensional super depth field microscope produced by Keyence. The laser scribing parameters adopted were the following: laser power of 50 W, pulsed laser frequency of 20 kHz, laser pulse duration of 45  $\mu\text{s}$ , laser beam radius of 0.02 mm, the overlapping rate of laser irradiated area is 99%, air pressure during blowing of 0.35 MPa, laser scribing speed of 4 mm/s, laser scanning number of 1 times.

## 3. Mathematical model and numerical simulation

The detailed assumptions were used to build the mathematical model can be seen in our previous paper [22]. The spatial distribution of the laser beam is in Gaussian at TEM<sub>00</sub> mode, the Gaussian laser intensity is  $3.68 \times 10^5$  W/mm<sup>2</sup>.

During laser scribing, the laser beam moves on the surface of the Al<sub>2</sub>O<sub>3</sub> sample with velocity  $V$ . The heat transfer equation can be expressed as [35]:

$$\rho c \frac{\partial T}{\partial t} = k \left( \frac{\partial^2 T}{\partial x^2} + \frac{\partial^2 T}{\partial y^2} + \frac{\partial^2 T}{\partial z^2} \right) + Q(x, y, z, t) \quad (1)$$

where  $\rho$  is the density,  $c$  is the heat capacity,  $k$  is the thermal conductivity, and  $T$  is the temperature of the ceramic sample.  $Q(x, y, z, t)$  represents the internal heat generation rate in the body. In this paper,  $Q(x, y, z, t) = Q_0(x, y, 0, t) = Q_0$  is the heat source term resembling the laser beam [1].

As the laser is capable to penetrate the alumina sample, its absorption is described as Beer–Lambert bulk absorption rather than surface absorption [36]. The laser heat source,  $Q_0$  can be treated as a heat production term and can be expressed as [1,35,37]:

$$Q_0 = \frac{2P}{\pi r^2} \cdot \frac{1}{(1 - e^{-2})} \cdot a \cdot e^{-az} (1 - r_f) e^{-\frac{x^2 + y^2}{r_0^2}} \quad (2)$$

where  $P$  is laser power,  $r$  is the laser beam radius,  $a$  is the absorption coefficient,  $r_f$  is the surface reflectivity [35], and  $r_0$  is the Gaussian parameter.

The initial condition is written as:

$$T(x, y, z, 0) = T_0 = 25^\circ C \quad (3)$$

In laser beam moving, the assisted gas flows through a coaxial nozzle towards the specimen surface. A convective flux is therefore used to define the boundary layer in correspondence of the top surface:

$$k \left( \frac{\partial T}{\partial x} n_x + \frac{\partial T}{\partial y} n_y + \frac{\partial T}{\partial z} n_z \right) = h_f (T_0 - T) \quad (4)$$

where  $h_f$  [35] is the forced convection heat transfer coefficient. With the exception of the plane of symmetry and of the bottom surface, the remaining boundary surfaces of the specimen exchange heat with the surrounding environment through natural convection. The corresponding boundary condition is expressed as:

$$k \left( \frac{\partial T}{\partial x} n_x + \frac{\partial T}{\partial y} n_y + \frac{\partial T}{\partial z} n_z \right) = h (T_0 - T) \quad (5)$$

where  $h$  is natural convection heat transfer coefficient.

The temperature distribution can be calculated by solving equations (1) – (5). The groove width and depth of laser scribing on specimen is identified as the portion of material in correspondence of which the temperature is higher than the melting temperature (2030°C) of  $Al_2O_3$ .

The laser beam moves along the surface of the  $Al_2O_3$  ceramics plate with trajectories that start from the same point and proceed along different angles. A three-dimensional finite element model was developed to describe the temperature field of the sample. The establishment of finite element model in this paper consists of six parts: unit type selection and mesh generation, determination of thermophysical properties of alumina ceramic materials, treatment of boundary conditions, heat source loading, and determination of time step.

According to the characteristics of laser sharp angle scribing, an eight-node hexahedral unit was selected (SOLID 70), and the surface unit (SURF 152) was used to load the forced convection coefficient. Due to the sharp corners, the use of the unit MESH 200 was necessary to partition the  $x$ - $y$  plane into quadrilaterals. To obtain the best compromise between accuracy of the result and computation time, the gradient mesh generation was used. A minimum mesh having size of  $0.01 \times 0.01 \times 0.046 \text{ mm}^3$  was used to

describe the region heated by the laser, while free meshing was applied to the remaining part of the sample. Finally, the SWEEP command was used to partition the entire volume.

The sample A model with an angle of  $15^\circ$  has 161661 hexahedron elements and 156816 nodes. The sample B model with an angle of  $60^\circ$  has 225978 hexahedron elements and 221089 nodes. It should be pointed out that laser scribing is a process in which the temperature varies sharply with time and space and there exists a strong temperature gradient in each space around the laser beam spot. In order to increase the efficiency and accuracy of the solution, dense meshes are divided in the laser heating region, while in the far away from the laser heating region, the temperature gradient is relatively small and the grid is coarse. In the actual mesh generation, the mesh density should be controlled according to the size of laser beam spot and the requirements of laser scribing geometry. It is generally required that the laser action region grid of the entity model should be less than or equal to  $1/2$  of the laser beam radius  $r$  [38], so the length of the grid element in this paper is taken as  $r/2$ , that is, 0.01 mm. The mapping grid method is adopted in the laser action zone, and the irregular body is far away from the laser action zone, and the free mesh method is adopted.

In the numerical simulation of laser scribing process, the thermal physical properties of the alumina ceramic materials are as follows: thermal conductivity  $k$ , specific heat capacity  $c$ , density  $\rho$ , melting point  $T$  and the initial temperature  $T_0$  of the alumina ceramic materials ( $25^\circ C$ ). For the sake of simplicity, the variation of material thermal properties with temperature is not considered in this paper.

The boundary conditions in this paper are the above equations (3) ~ (5).

Since the laser used in this paper is a pulsed laser, the pulsed laser scribing process can be divided into two stages (pulse action stage and pulse intermittent stage), then each loading step is divided into two parts. In pulse action stage, the position of the heat source center is changing with time. In this paper, the function of ANSYS is used to load the center of the heat source. In each load step, the center point of the heat source is taken as the center. According to the variation form of laser Gaussian bulk heat source (equation (2)), the position of the heat source center point in each load step changes correspondingly with the heat source moving. By controlling the position of the laser beam spot center, the laser beam spot changes with time, and the heat source can be moved. In the intermittent stage of pulsed laser, there is no effect of laser heat source. After removing the load of laser body heat source at the stage of pulse action, it can be calculated. In the intermittent stage, the temperature gradient of the laser scribing location is smaller, and the computation is easier to converge, which can increase the time step.

In the process of laser scribing, the laser beam spot moves continuously on the sample surface, and the load changes with time during loading, so it belongs to nonlinear analysis. In order to express the load varying with time, the load-time curve must be divided into load steps, and each inflection point in the load-time curve must be a load step. For each load step, the load value and the time value

must be defined. At the same time, it is necessary to select the load step by gradient or step (KBC=1). According to the linear heat transfer theory, the initial time step can be estimated according to formula  $ITSX=(\rho c/k)\times(\delta/2)^2$  [38], where  $\delta$  is the unit length of the maximum thermal gradient along the direction of heat flux. To ensure the stability and convergence of the calculation, the following settings are made: (1) Full Newton- Raphson method is adopted, which is characterized by that when each incremental iteration is solved, one equilibrium iteration is carried out and the heat balance matrix is modified. At the same time, the adaptive descent function is activated; (2) Turning on the prediction of time step because the setting of time step usually has a great influence on the calculation accuracy. The smaller the time step, the more accurate the calculation. In the pulse action stage, the time step of the load step should be controlled at about one pulse time, and the temperature will begin to decrease in the pulse intermittent stage before the method of variable step size can be considered and the time step can be increased.

Finally, the temperature field was simulated using the finite element software ANSYS APDL command flow. The parameters used in the simulations reported in this paper are given in Table 1 [36,39–41]. The computation times were around 76.8 and 104.2 h for samples A and B, respectively. When the laser scribing temperature field calculation process is finished, the all calculated temperature values can be outputted through the output program, and then the melting point figures of 3D view temperature more than alumina ceramic melting point (2030 °C) at different positions can be got with the use of ANSYS software. Finally, the laser scribing depth and width at different positions can be calculated according to the definition of laser scribing depth and width in this paper based on the melting point figures of 3D view temperature.

**Table 1** The simulated parameters

Calculating parameters	Values
Density $\rho$ (Kg/m <sup>3</sup> )	3720
Specific heat capacity C (J/Kg°C)	880
Thermal conductivity k (W/m°C)	25
Melting temperature T (°C)	2030
Forced convection heat transfer coefficient $h_f$ (W/m <sup>2</sup> °C)	3000
Natural convection heat transfer coefficient h (W/m <sup>2</sup> °C)	20
Reflectivity $r_r$	0.79
Absorption coefficient $a$ (1/m)	6000

**4. Results and discussion**

Fig. 1 shows the picking up temperature points of different samples which the distance between two points is 0.5mm. Fig. 2 and Fig.3 are the photographs of laser scribing width and depth of different samples at the corner, respectively. It should be pointed out that we use the method of applying force on the back of laser scribing samples to separate them mechanically, so as to obtain the laser scribing depth data and depth photographs at different positions in Fig.1. Of course, the laser scribing width and width photographs at different points in Fig.1 are measured and taken before mechanical separation, respectively. Both the width and depth of sample A are bigger than that of sample B. Specially, at the corner, the measured values of groove width are 0.064 mm for sample A and 0.054 mm for sample

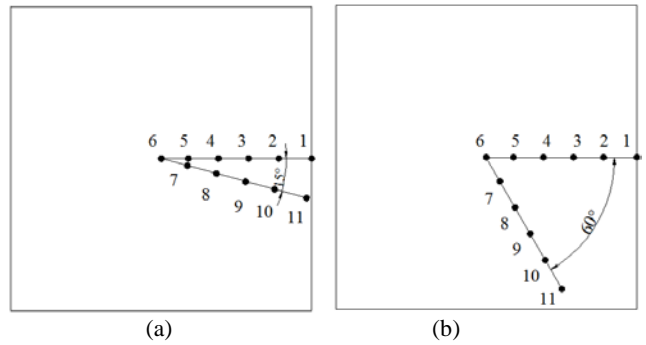


**Fig.1** Picking up temperature points for samples: (a) A and (b) B

B; the measured values of groove depth are 0.093 mm for sample A and 0.080 mm for sample B. The calculated maximum temperatures at different laser scribing lengths are given in Table 2. Three conclusions can be drawn from Table 2. First, it can be seen that with the increase of laser scribing length, the calculated maximum temperatures of different samples increase, which shows that there is thermal accumulation effect in the process of laser scribing. Second, the calculated maximum temperatures at the corner (corresponding to the laser scribing length of 2.5 mm) of different specimens are higher than that at both sides, which shows that there is sharp corner effect at the corner of laser scribing. Third, the calculated maximum temperature for sample A is higher than that of sample B, which

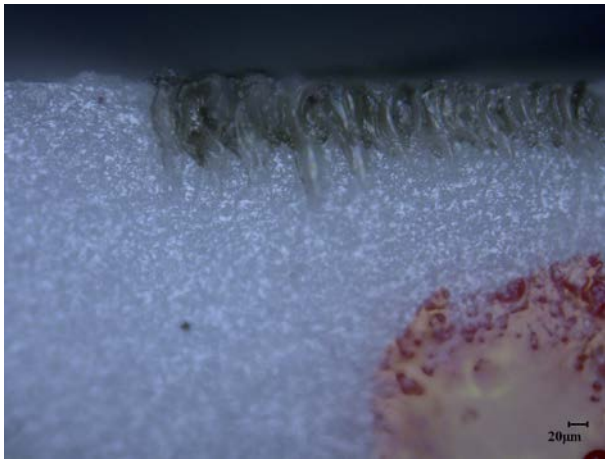


(a)

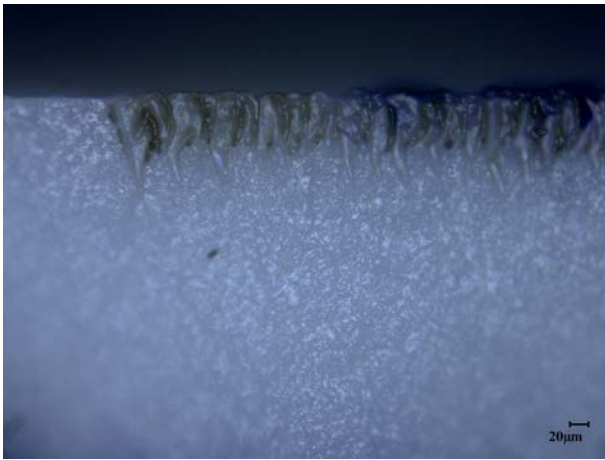


(b)

**Fig.2** Width photographs after laser scribing at the corner for samples: (a) A and (b) B



(a)



(b)

**Fig.3** Depth photographs after laser scribing at the corner for samples: (a) A and (b) B

**Table 2** Calculated maximum temperatures at different laser scribing lengths

Laser scribing length (mm)	Maximum temperature of sample A (°C)	Maximum temperature of sample B (°C)
0	2281.99	2276.65
1.25	2677.57	2311.89
2.5	2706.10	2532.21
3.75	2589.17	2512.21
5	3995.79	3262.25

shows that there is angle effect in the process of laser scribing.

In addition, there is a heat flux asymmetry phenomenon in the process of laser scribing sharp angle. To illustrate this problem, ten points marked as A1, A2, A3, A4, A5 (outer side) and B1, B2, B3, B4, B5 (inner side) were used, respectively, at two sides (0.1 mm) of the laser scribing path, as shown in Fig.4, where line CD is an angular bisector, and taking the sharp angle as the origin, the line CA3 is the negative axis, and the line B3D is the positive axis.

Fig. 5 shows the temperature distributions on angle bisector of different samples. From Fig.5, it can be seen that the inner side temperature TB (positive half axis) is higher than that of outer side TA (negative half axis) at the same distance for different samples. This indicates that heat flux asymmetry phenomenon exists at the sharp corner.

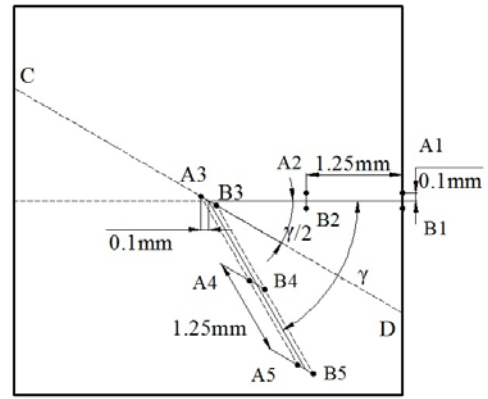
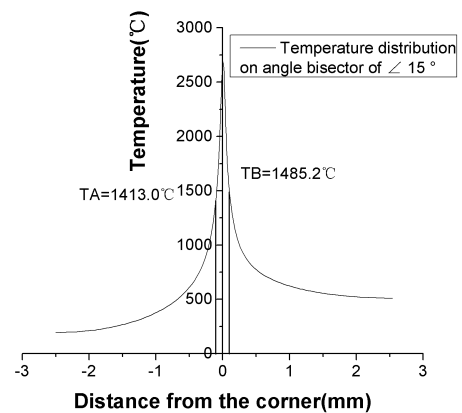
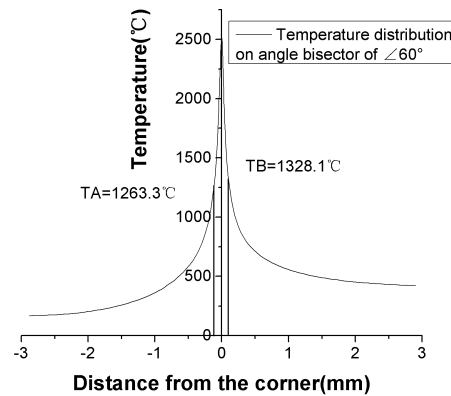


**Fig.4** Picking up temperature points for heat flux asymmetry phenomenon



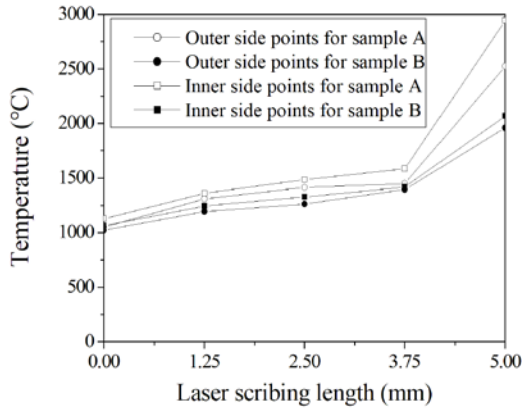
(a) Sample A



(b) Sample B

**Fig.5** Temperature distributions on angle bisector of different samples

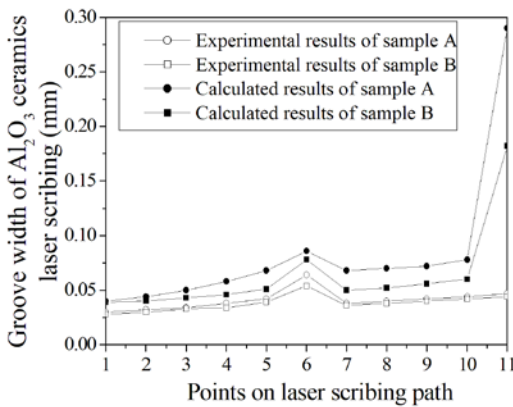
Fig. 6 gives the inner and outer sides temperature distributions of different samples. It can be seen that the temperatures at inner and outer sides at the same laser scribing length are different; the inner side temperatures are higher than that of outer side for sample A and sample B; the inner and outer side temperatures of sample A are higher than that of sample B. This shows that heat flux asymmetry phenomenon exists in the laser scribing process for sharp angle, and the smaller the sharp angle, the more serious the asymmetry of heat flux.



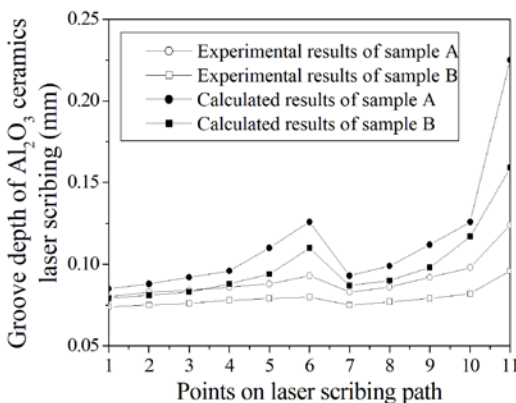
**Fig.6** Inner and outer side temperature distributions of different samples

Fig.7 and Fig.8 are the comparison of the groove width and depth for different samples based on experimental results and calculated results, respectively.

First, it can be seen that the experimental results are consistent with the trend of the calculated results. With the increase of laser scribing length from position points 1 to 11, the groove width and depth for both samples increases.



**Fig.7** Comparison between experimental results and calculated results of groove width for different samples



**Fig.8** Comparison between experimental results and calculated results of groove depth for different samples

This is mainly due to heat accumulation effect (Table 2, Fig.9 and Fig.10). This phenomenon has been reported in laser ceramic scribing straight path [22,42]. Specially, the

measured values of groove width increased from 0.030 mm to 0.047 mm for sample A and from 0.028 mm to 0.044mm for sample B; the measured values of groove depth increased from 0.080 mm to 0.124 mm for sample A and from 0.074 mm to 0.096 mm for sample B. Corresponding to this is that the calculated values of groove width increased from 0.040 mm to 0.290 mm for sample A and from 0.039 mm to 0.182 mm for sample B; the calculated values of groove depth increased from 0.085 mm to 0.225 mm for sample A and from 0.079 mm to 0.159 mm for sample B. It should be noted that the differences between the calculated results and the experimental results increase with the increase of laser scribing length, which may be related to many factors such as mathematical model assuming, without considering the thermos-physical parameters of alumina ceramics changing with the variation of temperature, without considering thermal radiation, without considering convection heat transfer coefficient ( $h$  and  $h_f$ ), reflectivity  $r_f$  and absorption coefficient  $\alpha$  changing with temperature etc.. These will be considered in subsequent research.

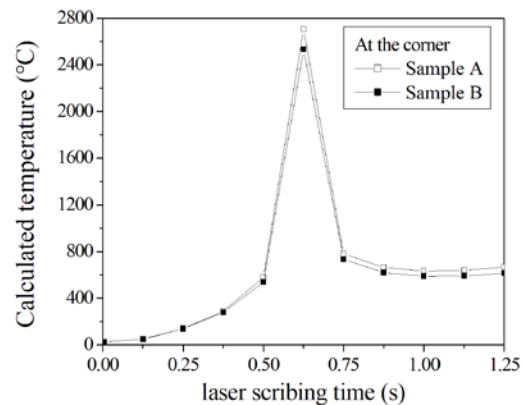


**Fig.9** Calculated temperature change of different samples at the fixed sharp corner position and  $Z=0$  mm after laser scribing 1 times

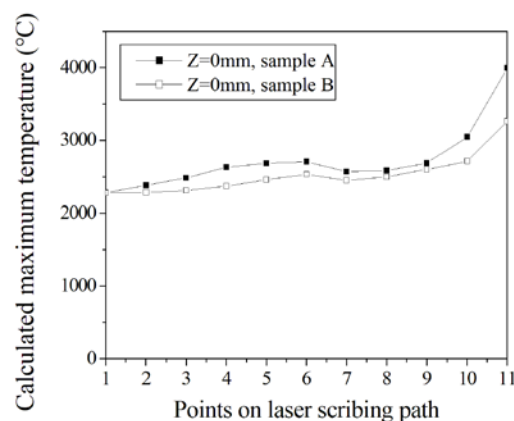


**Fig.10** Calculated maximum temperature of different samples at different positions after laser scribing 1 times

Second, it can be seen that when the sharp angle decreases from  $60^\circ$  to  $15^\circ$ , the groove width and depth of laser scribing increases. This is mainly due to angle effect (Table 2, Fig.9 and Fig.10). The size of the angle has important effect on heat accumulation effect of laser scribing.

The smaller the angle, the higher the temperature (Table 2, Fig.9 and Fig.10), resulting in the increase of groove width and depth of laser scribing (Fig.7 and Fig.8).

Third, it can be seen that the groove width and depth of laser scribing at the corner (2.5 mm, position point 6) is bigger than that of its two sides (position point 5 and position point 7). Specially, the measured values of groove width of position points 5,6,7 are 0.042 mm, 0.064 mm and 0.038 mm for sample A, respectively; the measured values of groove width of position points 5,6,7 are 0.039 mm, 0.054 mm and 0.036 mm for sample B, respectively. The measured values of groove depth of position points 5,6,7 are 0.088 mm, 0.093 mm and 0.083 mm for sample A, respectively; the measured values of groove depth of position points 5,6,7 are 0.079 mm, 0.080 mm and 0.075 mm for sample B, respectively. Corresponding to this is that the calculated values of groove width of position points 5,6,7 are 0.068 mm, 0.086 mm and 0.068 mm for sample A, respectively; the calculated values of groove width of position points 5,6,7 are 0.051 mm, 0.078 mm and 0.050 mm for sample B, respectively. The calculated values of groove depth of position points 5,6,7 are 0.110 mm, 0.126 mm and 0.093 mm for sample A, respectively; the calculated values of groove depth of position points 5,6,7 are 0.094 mm, 0.11 mm and 0.087 mm for sample B, respectively. This phenomenon can be explained by sharp corner effect. Specially, when an angle shape is scribed using laser beam, the direction of heat flux will change during the laser beam approaching and leaving the sharp corner. In addition, the areas of the inner and outer sides of the sharp corners are different, and the inner heat dissipation area of the corner is smaller than that of the outer. Therefore, the degrees of heat dissipation to the two sides at the corner are different, this is called "heat flux asymmetry" phenomenon (Fig.5). The temperature decreased a little after the position point 6 (Fig.10). Passing through the sharp corner (position point 6), the asymmetry of the heat flux gradually restored. So, with the increase of laser scribing time, heat accumulation effect continues to strengthen again, resulting in the increase of the groove width and depth of laser scribing again (Fig.7 and Fig.8). Obviously, the heat accumulation effect at the corner is stronger, the groove width and depth of laser scribing is larger than that of both sides (Fig.7 and Fig.8).

Fourth, for the laser scribing depth and width of different samples, both the calculated value and the experimental value all start to appear small (corresponding to laser scribing length of 0~0.5 mm), then slowly increase (corresponding to laser scribing length of 0.5~4.5 mm), and finally increase sharply (corresponding to laser scribing length of 4.5~5.0 mm). This may be related to the heat transfer characteristics of laser scribing limited size objects.

In fact, for any laser processing technology, when a specific finite size object is heated by a laser, there are three stages in the process of laser heating, that is, the onset stage of the underheating, the intermediate stage of heat balance and the last stage of overheating. For a given corner angle laser scribing, the thermal heat at the three locations named the laser scribing start edge, the laser scribing middle of the part and the laser scribing end edge will increase subsequently. Specifically, in Fig.10, the calculated maximum temperatures are 2281.99°C for sample A and

2276.65°C for sample B at the beginning stage (corresponding to laser scribing length of 0 mm and  $Z=0$  mm); the calculated maximum temperatures are 2381.74 °C ~3044.67 °C for sample A and 2284.9°C ~2714.28 °C for sample B in the middle stage (corresponding to laser scribing length of 0.5~ 4.5mm and  $Z=0$  mm); the calculated maximum temperatures of the final stage (corresponding to laser scribing length of 4.5~5.0mm and  $Z=0$  mm) are 3995.79°C for sample A and 3262.25°C for sample B. The start edge is less heated by laser due to lack of pre-heating (Heat dissipation is greater than heat accumulation); the laser spot ahead in the middle of the laser scribing part has been pre-heated by the laser itself during laser scribing and there the heat has been balanced (Heat dissipation is almost equal to the amount of heat accumulation); the end edge was over-heated by heat accumulation (Heat dissipation is less than heat accumulation) because there is no physical conduct to transfer the laser heat away at the end edge. So, the laser scribing depth and width are smaller at the start edge region (Fig.7 and Fig.8, corresponding to laser scribing length of 0~0.5 mm), almost constant at the laser scribing middle region (Fig.7 and Fig.8, corresponding to laser scribing length of 0.5~4.5 mm) and larger at the end edge region (Fig.7 and Fig.8, corresponding to laser scribing length of 4.5~5.0 mm).

In addition, it is well known that the phenomena and mechanism of interaction between laser and matter for the long pulse laser such as the microsecond laser and the ultrashort pulse laser such as the femtosecond laser is different. The former belongs to thermodynamic process and the latter belongs to non-thermodynamic process [43]. Since the pulse width of the microsecond laser is much larger than the time of thermal diffusion, when the microsecond pulse laser acts on the material, the material is mainly melted, vaporized and removed by means of thermal energy. Therefore, the formation mechanism of the groove depth and width also involves the melting and vaporization in the laser scribing alumina ceramic process in this paper. However, since the boiling point of alumina is 2980 °C, according to Table 2, the evaporation process mainly occurs in the last stage of laser scribing. In other words, during the laser scribing process in this paper, the melting - removal mechanism is mainly in the early and middle stages of laser scribing.

## 5. Conclusions

- (1) The corner angle has a significant effect on groove width and depth on  $Al_2O_3$  due to the heat accumulation effect and the corner angle effect. The effect is more evident for smaller corner angle.
- (2) Heat flux asymmetry phenomenon exists in the laser scribing process for corner angle.
- (3) The experimental results are consistent with the trend of the calculated results.

## Acknowledgments

This work was supported by Open Research Fund Program (XDKFJJ[2016]06) of Key Laboratory of Advanced Manufacturing Technology, Ministry of Education, Guizhou University, Open Research Fund Program (LZSY-01) of Zhejiang Provincial Key Laboratory of Laser Pro-

cessing Robot/ Key Laboratory of Laser Precision Processing & Detection, Wenzhou University, Open Research Fund Program (9T-12006) of Shaanxi Key Laboratory of Non-Traditional Machining, Xi'an Technological University, and the Fund (SKLSP201733) of the State Key Laboratory of Solidification Processing in NWPU. The authors are also grateful to Analytical and Testing Center of Huazhong University of Science and Technology.

## References

- [1] B.S. Yilbas, S.S. Akhtar, and C. Karatas: *Mach. Sci. Technol.*, 18, (2014) 424.
- [2] B.S. Yilbas, S.S. Akhtar, and O. Keles: *Int. J. Adv. Manuf. Tech.*, 79, (2015) 101.
- [3] J. Hildenhagen, U. Engelhardt, M. Smarra, and K. Dickmann: *Proc. of Frontiers in Ultrafast Optics: Bio-medical, Scientific, and Industrial Applications XII*, San Francisco, (2012), p.824711.
- [4] M.F. Trubelja, S. Ramanathan, M.F. Modest, and V.S. Stubican: *J. Am. Ceram. Soc.*, 77, (1994) 89.
- [5] Y. Iwai, T. Mizuno, T. Arai, T. Honda, R. Tanaka, and T. Takaoka: *Proc. 4th International Symposium on Laser Precision Microfabrication*, Munich, (2003), p.509.
- [6] M. Takahashi, Y. Kurihara, K. Yamada, K. Kanai, and K. Kurihara: *Electron. Comm. Jpn.* 2., 73, (1990) 105.
- [7] J.K. Lump, and S.D. Allen: *IEEE Trans. Compon., Packag. Manuf. Technol., Part B: Adv. Packag.*, 20, (1997) 241.
- [8] C.H. Tsai, and H.W. Chen: *J. Mater. Process. Tech.*, 136, (2003) 166.
- [9] X. Z. Xie, X. D. Huang, W. F. Chen, X. Wei, W. Hu, and R. H. Che: *Chin. J. Lasers*, 40, (2013)1203010-1. (in Chinese)
- [10] T. C. Chen, and R.B. Darling: *J. Mater. Process. Tech.*, 169, (2005)214.
- [11] Y. Iwai, T. Arai, T. Honda, R. Tanaka, and T. Takaoka: *Proc. 3th International Symposium on Laser Precision Microfabrication*, Osaka, (2002), p.110.
- [12] J. Y. Xu, H. Hu, C. H. Zhuang, G. D. Ma, J. L. Han, and Y. L. Lei: *Opt. Laser. Eng.*, 102, (2018)26.
- [13] C.H. Tsai, and H.W. Chen: *Int. J. Adv. Manuf. Technol.*, 23, (2004) 342.
- [14] G. David: *Hybrid Circuit Technol.*, 8, (1991) 30.
- [15] Y. Iwai, T. Arai, T. Honda, R. Tanaka, and T. Takaoka: *Proc. 4th International Symposium on Laser Precision Microfabrication*, Munich, (2003), p.362.
- [16] M. Passler, and G. Lensch: *Proc. High Power Lasers: Sources, Laser-Material Interactions, High Excitations, and Fast Dynamics in Laser Processing and Industrial Applications*, Hague, (1987), p.283.
- [17] M.A. Saifi, and R. Borutta: *Am. Ceram. Soc. Bull.*, 54, (1975) 986.
- [18] K.G. Xia: "Experimental study on laser processing of ceramic substrate" [D], Shandong: Yantai University, 2009, p.41-49. (in Chinese)
- [19] M.F. Modest, and T.M. Mallison: *J. Heat Trans.*, 123, (2001) 171.
- [20] U.C. Paek, and V. J. Zaleckas: *Am. Ceram. Soc. Bull.*, 54, (1975) 585.
- [21] Z.G. Xu, C.S. Xu, L. Ha, and R.H. Zhou: *Applied Mechanics and Materials*, 217-219, (2012) 2265.
- [22] K.J. Huang, S. Wang, and L. Tang: *Mater. Res. Innov.*, 19, (2015) 239.
- [23] K.J. Huang, S. Wang, X. Chen, H.S. Huang, S.H. Tang, and F.L. Du: *J. Laser Micro Nanoen.*, 13, (2018)10.
- [24] B.S. Yilbas, A.F.M. Arif, and B.J.A. Aleem: *Opt. Laser Eng.*, 48, (2010)10.
- [25] B.S. Yilbas, S.S. Akhtar, and C. Karatas: *Opt. Laser Eng.*, 55, (2014)35.
- [26] Q.S. Deng, C.F. Zhao, L. Chen, M.G. Shi, W.H. Yang, and X.H. Tang: *Chin. J. Lasers*, 39, (2012)0803006-1. (in Chinese)
- [27] W.C. Wu: "Modeling and analysis of thermal stress field for laser cutting corner in steel sheet" [D], Shanghai: Shanghai Jiao Tong University, 2013, p.80-95. (in Chinese)
- [28] J. Zhou, and C.Y. Yu: *Aeronautical Manuf. Technol.*, 5, (1991)9. (in Chinese)
- [29] B.S. Bilbas, A,F,M,Arif, and B.J.A. Aleem: *J. Mater. Eng. Perform.*, 19, (209)177.
- [30] J. Seebach, S. Norman, and P. Harrison: *Proc. 4th Industrial Laser Applications Symposium*, Kenilworth, (2015), p.965706.
- [31] D.G. Ahn, and H.J. Park: *Key Eng. Mater.*, 344, (2007)169.
- [32] Q. Li: "Some research on laser micromachining applied in electronic industry" [D], Hangzhou: Zhejiang University, 2010, p.68-72. (in Chinese)
- [33] C. Wang, and X.Y. Zeng: *Laser Technol.*, 31, (2007)18. (in Chinese)
- [34] J. A Todd, and S.M. Copley: *J. Manuf. Sci. E. -T. ASME*, 119, (1997)55.
- [35] B.S. Yilbas, S.S. Akhtar, and C. Karatas: *Int. J. Adv. Manuf. Tech.*, 58, (2012) 1019.
- [36] Y.Z. Yan: "Investigation on laser crack-free cutting of ceramics" [D], Beijing: Beijing University of Technology, 2013, p.56-57. (in Chinese)
- [37] W.P. Wang, B.D. Lu, and S.R. Luo: *High Power Laser Part. Beams*. 13, (2001) 313. (in Chinese)
- [38] Q.F. Zheng: "Research on laser processing fracture splitting groove technology and automation equipment for engine connecting-rod" [D], Changchun: Jilin University, 2010, p.55-60. (in Chinese)
- [39] Y.L. Zhang and J.P. Ma: "Practical handbook of ceramic materials", (Chemical Industry Press, Beijing, 2006 )p.343. (in Chinese)
- [40] Blake William Clark Sedore: "Laser welding of alumina ceramic substrates with two fixed beams" [D], Kingston: Queen's University, 2013, p.58.
- [41] E. Kacar, M. Mutlu, E. Akman, A. Demir, L. Candan, T. Canel, V. Gunay, and T. Simmazcelik: *J. Mater. Process. Tech.*, 209, (2009) 2008.
- [42] D.W. Wang, and X.F. Gao: *Chin. J. Lasers*, 42, (2015) 0303005-1. (in Chinese)
- [43] X.C. Zheng: "Study on preparation of black silicon by microsecond pulsed laser" [D], Hangzhou: Zhejiang University, 2014, p.25-26. (in Chinese)

(Received: May 23, 2018, Accepted: October 9, 2018)